Ligand Dissociation and Core Fission from Diphosphine-Protected Gold Clusters

ARTICLE *in* THE JOURNAL OF PHYSICAL CHEMISTRY C · JUNE 2007

Impact Factor: 4.77 · DOI: 10.1021/jp0712811

2 AUTHORS:

Denis E Bergeron
National Institute of Standards and Technolo…
55 PUBLICATIONS **884** CITATIONS
SEE PROFILE

Jeffrey W Hudgens
National Institute of Standards and Technolo…
136 PUBLICATIONS **2,342** CITATIONS
SEE PROFILE

Ligand Dissociation and Core Fission from Diphosphine-Protected Gold Clusters

Denis E. Bergeron and Jeffrey W. Hudgens*

National Institute of Standards and Technology, Gaithersburg, Maryland 20899

Received: February 14, 2007; In Final Form: April 5, 2007

Highly monodisperse samples of diphosphine ligand (1,3-bis(diphenylphosphino)propane- or 1,5-bis-(diphenylphosphino)pentane)-protected gold nanoparticles form rapidly in a mixed methanol/chloroform solvent environment. Methanol soluble octagold, decagold, and undecagold monolayer protected clusters yield very stable ion currents when introduced into a mass spectrometer via electrospray ionization. In addition to neutral ligand loss pathways, collision-induced dissociation generates $[AuL]^+$ and $[Au_3L]^+$ (L = diphosphine ligand) as particularly stable product ions from all clusters considered. Furthermore, deca- and undecagold clusters are found to be more resistant to collision induced dissociation, and more susceptible to partial ligand losses than octagold clusters. This suggests that for the deca- and undecagold species, Au−P and P−Ph (Ph = phenyl) bonds within the ligand-protected clusters are of comparable strength.

1. Introduction

In addition to being technologically interesting in their own right, small monolayer-protected gold clusters (MPCs) offer a glimpse at the evolution of embryonic nanoparticles, and may ultimately enable researchers to establish the principles necessary for more exact syntheses. Monodispersity is critical for many applications in nanotechnology, ranging from optoelectronic to biomedical. The formation of MPCs is governed by complicated but ideally tractable thermodynamic and kinetic factors, in principle allowing for the manipulation of reaction conditions toward a predetermined size (or size distribution).[1] Recent efforts to unravel the mechanisms involved in the emergence of embryonic nanoparticles have shown the promise of applying mass spectrometric techniques to the problem.[2]

Mass spectrometry is not new to nanoparticle research, as matrix-assisted laser desorption ionization (MALDI) and—less commonly—electrospray ionization (ESI) sources have enabled nanoparticles to be subjected to mass spectrometric analysis.[2−14] However, in most cases the analysis is restricted to determining the size and monodispersity of the particles. The complete arsenal of mass spectrometric techniques regularly utilized in proteomics and cluster science has not been brought to bear on problems associated with MPCs. This is at least partially due to the predominance of MALDI, which does not couple to compound instruments as easily as ESI, making tandem mass spectrometric experiments such as collision induced dissociation (CID) more difficult. ESI not only enables facile coupling to compound instruments, but also facilely produces multiply charged ions so that the *m*/*z* of many nanoparticles falls into a range easily accessed by commercial instruments. A recent study has taken advantage of these properties to investigate MPCs.[2]

Two different classes of MPCs have been investigated via ESI, each with fundamentally different intrinsic charge characteristics. As Whetten and others have demonstrated, thiol protected clusters with easily deprotonated ligands (such as polypeptides) enable the study of multiply charged clusters.[4,6−12,14] In contrast, several small Au clusters, most notably undecagold, tend toward a charged Au core, so that multiply charged clusters can be realized in an ESI setting, thus eliminating the necessity for easily (de)protonated ligands.[2,13,15] Recently, Bertino et al. reported a facile synthesis of octa-, deca-, and undecagold clusters and analysis via ESI mass spectrometry (ESI-MS).[13] These very small species offer the advantage of decades of study by inorganic chemists, often including structures determined via X-ray crystallography.[16,17]

Herein, we describe findings on the solubility properties of the clusters reported by Bertino et al.[13] The choice of solvent environment proves a useful tool for the generation of desired products, and we are able to simplify the synthetic procedure of Bertino et al.[13] while speeding up the reaction, extending shelf life, and producing more stable ion currents via ESI. Stable ion currents enabled us to perform CID experiments, and we address the fragmentation patterns observed, particularly emphasizing motifs recurrent for the three clusters considered. In light of the CID results, we address the structural implications of our observation that gold core fission represents an important fragmentation mechanism for these small clusters.

2. Experiment

2.1. UV−Vis Spectroscopy. UV−vis spectra were collected with a dual beam Varian Cary 3C UV−vis spectrophotometer.[18] The strong undecagold absorption at ≈ 420 nm served as a benchmark in the present studies and is consistent with previous reports for undecagold.[11,13,17] Solutions containing octa- and decagold clusters were identified by the peak at ≈ 415 nm, as well as the extended shoulder to the red, as per the report of Bertino et al.[13]

2.2. ESI MS/MS. Mass spectra were obtained using a Micromass Quattro Micro triple quadrupole instrument. A range of drying temperatures and cone voltages were scrutinized, so that optimal signal intensity and stability could be achieved with minimal fragmentation. Selected ions were introduced into a collision cell with 1.6 mTorr Ar as a collision gas, and MS/MS spectra were measured over a range of collision energies. The *m*/*z* range of the spectrometer extended up to 2000, so that multiply charged clusters were easily observed and assigned based on previous reports and isotopic analyses. When specific clusters were mass-selected for CID, charge loss could lead to

* Corresponding author. E-mail: hudgens@nist.gov.

10.1021/jp0712811 CCC: $37.00
Published on Web 05/19/2007

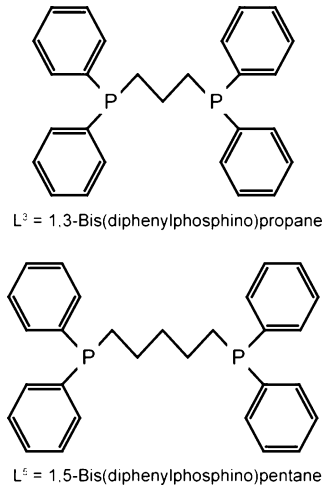

Figure 1. The two diphosphine ligands employed in the syntheses.

product ions with *m*/*z* values in excess of our experimental limit of 2000. However, in such cases, complementary product ions were observed, so that the presence of the high *m*/*z* product ion could be inferred. Spectra were typically acquired in "centroid" mode, so that signals within individual time intervals were centered and integrated by the instrument data system. When isotopic analysis was necessary to determine the charge state of a particular *m*/*z* peak, the instrument was run in "continuous" mode.

2.3. Cluster Synthesis and Characterization. Figure 1 depicts the two ligands employed in the current studies. Synthesis of the $[Au_{11}L^3_5]^{3+}$ cluster was previously achieved via ligand exchange[16] and, more recently, via direct synthesis in chloroform.[13] In the present work, we first synthesized the clusters according to the recipe described by Bertino et al.[13] In short, 0.1 mmol of $Au(PPh_3)Cl$, 0.1 mmol of 1,3-bis(diphenylphosphino)propane (L^3), and 0.5 mmol of borane tert-butylamine complex, a weak reducing agent,[19] were dissolved in 100 mL of $CHCl_3$ through which N_2 had been bubbled to displace any dissolved oxygen. The solution remained clear for several hours before a pale yellowish tint was observed. After 8 h, the color of the solution deepened to an orange-brown. UV−vis and ESI-MS confirmed the formation of $[Au_{11}L^3_5]^{3+}$ (vide infra), as has been described previously.[13] However, we repeatedly observed—particularly upon cessation of stirring—that a reddish precipitate formed in the reaction vessel. It was possible to filter this precipitate and wash it with $CHCl_3$. The filtrate was still orangish in color, containing $[Au_{11}L^3_5]^{3+}$, and we turned our attention to the precipitate.

We discovered that while the precipitate was insoluble in $CHCl_3$ and in water, it was very soluble in methanol (MeOH). UV−vis and ESI-MS analysis confirmed the presence of $[Au_{11}L^3_5]^{3+}$ in the MeOH solution. Furthermore, over time, further precipitate formed from the filtered $CHCl_3$ solution. We were thus convinced that the cluster (and/or its emergent salt) was far more soluble in MeOH than in $CHCl_3$. The details of this solvation behavior and its significance are addressed below.

We conducted a series of studies to establish what effects the presence of MeOH in the reaction solution might exhibit. Reactions were performed with as-delivered $CHCl_3$, under ambient lab conditions in a beaker with a stir bar (the less exacting conditions had no qualitative deleterious effects). We ultimately found that a 1:1 MeOH:$CHCl_3$ reaction solution turned pale yellow almost instantaneously and orange within about 10 min. In fact, the reaction could be performed (and more quickly than in pure $CHCl_3$) in pure MeOH, despite the fact that the reactants are relatively insoluble. Qualitatively, the ratio of the solvents appeared to have little effect on the products, and so the 1:1 solution, which enabled complete dissolution of both the reactants and the products, was found to be a convenient medium. Note that we did not perform any comparative studies to determine the effects of mixed solvent on yield or purity, as our primary interest involves preparing a sample for ESI interrogation of the product clusters.

By replacing L^3 with 1,5-bis(diphenylphosphino)pentane (L^5), we were also able to generate samples of the octa- and decagold sample described by Bertino et al.[13] Once again, by performing the reactions in a mixed MeOH/$CHCl_3$ solvent environment, the synthesis time was reduced significantly without any qualitative change to the products. The identity of the clusters was established by UV−vis and ESI-MS, and we note that the ratio of $[Au_8L^5_4]^{2+}$ to $[Au_{10}L^5_4]^{2+}$ in our mass spectra is similar to that reported by Bertino et al. While instrumental differences and solvent conditions make direct comparisons unreliable, the spectra seem to indicate the proportion of $[Au_8L^5_4]^{2+}$ is greater in our sample than in that of Bertino et al., and that the proportion of $[Au_9L^5_4]^{2+}$ in our sample is slightly smaller.

Storage in MeOH also had a positive effect on the clusters' shelf life. Clusters synthesized and stored in $CHCl_3$ were found to decompose over time when stored under air at room temperature; in one case, an orange undecagold solution stored in a sealed plastic sample bottle for ∼1 week absorbed enough oxygen to collapse the bottle. The solution became clear in the process. Under identical conditions, samples stored in MeOH did not succumb to any discernible decomposition within the extended time frame (∼8 weeks) of our investigations.

3. Results

3.1. Electrospray Mass Spectra. We found that clusters dissolved in MeOH generally yielded stronger and more stable ion currents than samples dissolved in $CHCl_3$. Figure 2 shows raw mass spectra obtained via direct infusion of three different samples. Figure 2a corresponds to a sample synthesized in $CHCl_3$, as reported by Bertino et al.[13] Here, a low cone voltage is used to minimize CID at the source. $[Au_{11}L^3_5]^{3+}$ is the most abundant cluster, but certainly does not represent the most intense peak in our spectra. We do see several of the small singly charged Au_x:L_y complexes mentioned by Bertino et al.,[13] but our spectrum does not feature the clean landscape (dominated by the $[Au_{11}L^3_5]^{3+}$ peak at *m*/*z* 1409) reported in their work.[20] Further, where using the $CHCl_3$ solvent environment for direct infusion to the electrospray source, we found that the ion current was very erratic, complicating the determination of peak ratios, and prohibiting MS/MS experiments.

Figure 2b shows the spectrum obtained with a sample prepared by dissolving in MeOH the red precipitate from a $CHCl_3$ solution. Collected under identical source conditions as in Figure 2a, the spectrum is now significantly cleaner and exhibits more ion intensity in the higher *m*/*z* range. The $[Au_{11}L^3_5]^{3+}$ cluster peak is dominant. A few singly charged $[Au_xL^3_yCl_n]^+$ species are present at lower *m*/*z*, and the $[Au_2L^3_2]^{2+}$ ion (assignment confirmed by isotope analysis) discussed by Colton et al.[21] makes a significant contribution. What is important to note here is that the cluster of interest, $[Au_{11}L^3_5]^{3+}$, now constitutes a major peak in the spectrum, and—even more importantly for CID studies—yields very stable ion current.

Figure 2c, which was obtained with a sample synthesized in a 1:1 MeOH:$CHCl_3$ solution and subsequently dried and redissolved in MeOH, was again collected under identical source conditions. In this sample, the $[AuL^3_2]^+$ ion dominates the mass

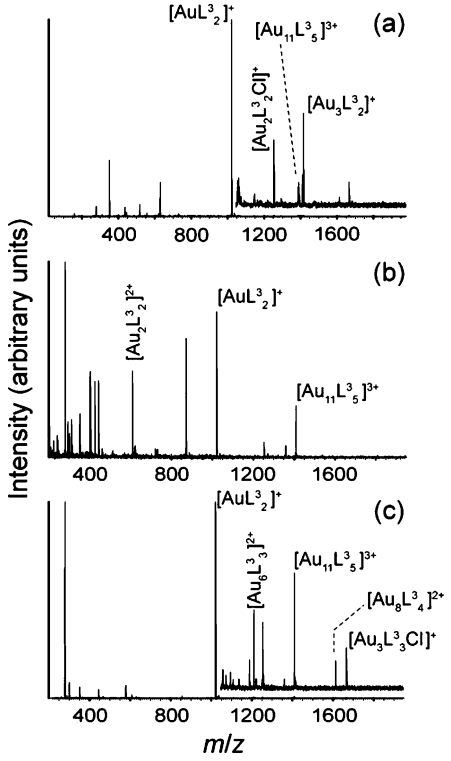

Figure 2. ESI Mass spectra of $[Au_{11}L^3_5]^{3+}$ samples collected by (a) synthesis in chloroform, (b) precipitation from chloroform, followed by dissolution in methanol, and (c) synthesis in a 1:1 methanol:chloroform solution. The high *m*/*z* range is magnified in panels a and c so that the clusters are visible.

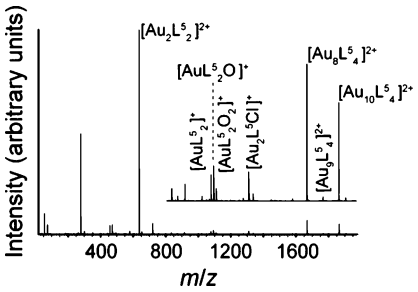

Figure 3. ESI Mass spectrum of $[Au_8L^5_4]^{2+}$ and $[Au_{10}L^5_4]^{2+}$ synthesized in a 1:1 methanol:chloroform solution.

spectrum, and the $[Au_2L^3_2]^{2+}$ ion is absent. The $[Au_{11}L^3_5]^{3+}$ ion (*m*/*z* 1409) is still a major contributor to the higher *m*/*z* region of the distribution, and its ion current is very stable, allowing for CID experiments. In addition, the magnified portion of the spectrum contains other cluster compounds, namely $[Au_6L^3_3]^{2+}$ and $[Au_8L^3_4]^{2+}$. We will return to the emergence of these clusters under the mixed-solvent reaction conditions in section 4.

Finally, we turn to the $[Au_xL^5_y]^{z+}$ clusters shown in Figure 3. The sample employed to collect this mass spectrum was synthesized in a 1:1 MeOH:$CHCl_3$ solution and subsequently dried and redissolved in MeOH. The most intense peak corresponds to the $[Au_2L^5_2]^{2+}$ ion, and several small $[Au_xL^5_y]^+$ clusters, in some cases associated to Cl or O,[21] are present. The three clusters reported by Bertino et al.[13] ($[Au_8L^5_4]^{2+}$, $[Au_9L^5_4]^{2+}$, and $[Au_{10}L^5_4]^{2+}$) are found to dominate the high *m*/*z* portion of the spectrum, with the enneanuclear (Au_9) component being the least abundant. Very stable ion currents were achieved, enabling CID of the octa- and decanuclear clusters.

3.2. CID Characteristics of Selected Ions. Using samples dissolved in MeOH, we were able to collect CID data for $[Au_8L^5_4]^{2+}$, $[Au_{10}L^5_4]^{2+}$, and $[Au_{11}L^3_5]^{3+}$ parent clusters delivered to the mass spectrometer via ESI. We shall discuss each in turn, paying particular attention to three major fragmentation pathways that recur for multiple clusters:

$$[Au_xL_y]^{z+} \xrightarrow{Ar} [Au_xL_{y-1}]^{z+} + L \quad (1)$$

$$[Au_xL_y]^{z+} \xrightarrow{Ar} [Au_{x-1}L_{y-1}]^{(z-1)+} + [AuL]^+ \quad (2)$$

$$[Au_xL_y]^{z+} \xrightarrow{Ar} [Au_{x-3}L_{y-1}]^{(z-1)+} + [Au_3L]^+ \quad (3)$$

These major pathways involve neutral ligand loss (eq 1), and two distinct core fission pathways (eqs 2 and 3). Under our multiple collision conditions, sequential fragmentation events are possible, so that the values of *x* and *y* do not always correspond to the values of the selected parent cluster. In addition, pathways involving partial ligand losses are seen. The exact fragmentation pathways for each cluster are discussed below, but two typical examples are given in eqs 4 and 5:

$$[Au_{11}L^3_5]^{3+} \xrightarrow{Ar} [Au_{11}L^3_4(Ph)P(CH_2)_3]^{3+} + PPh_3 \quad (4)$$

$$[Au_{10}L^5_4]^{2+} \xrightarrow{Ar} [Au_9L^5_3(Ph)_2P]^+ + [Au(Ph)_2P(CH_2)_5]^+ \quad (5)$$

Equation 4 describes a typical fragmentation event in which a neutral portion of a ligand is dissociated. Equation 5 describes a typical fragmentation event in which one gold atom and a portion of a ligand dissociate from the parent cluster and the charge is split between the two fragments.

The apparatus employed in these experiments afforded observations between *m*/*z* 20−2000. For fragmentation pathways described by eqs 1 and 4, all product ions fall within this range; however, product ions formed via the processes described in eqs 2, 3, and 5 have lower charge than the parents, so that their *m*/*z* values may exceed the range of our apparatus. In such cases, the presence of these product ions may be inferred by the observation of their complementary ions. For the observed product ions, Figure 4 depicts the major fragmentation channels as branching ratios. Tables S1−S3 include typical raw data.

3.2.1. $[Au_8L^5_4]^{2+}$. CID spectra of $[Au_8L^5_4]^{2+}$ exhibit relatively few product ions. Neutral ligand loss (eq 1), leaving $[Au_8L^5_3]^{2+}$, represents the most abundant product ion, starting at low collision energies, and persisting through the range studied here. Also appearing at low collision energies is the $[AuL^5]^+$ product ion (via eq 2). Note that the peak at *m*/*z* 637 can correspond to any $[Au_nL^5_n]^{n+}$ cluster, and in the distribution of nascent electrosprayed cluster ions (Figure 3) is assigned as $[Au_2L^5_2]^{2+}$. We performed isotopic analyses to distinguish different values of *n*, so that we are certain that the nascent cluster distribution contains the dimer dication, while the CID spectra contain singly charged $[AuL]^+$ product ions.

At a collision energy of ∼17 V, as the neutral ligand loss product ion begins to decay, a sharp rise is evident in the contribution of $[AuL^5]^+$ to the total ion current (TIC). At the same time, a new product ion, assigned as $[Au_3L^5]^+$ appears. This ion could only arise as the product of fission of the cluster core (eq 3), and so it is logical that it only occurs after the initial neutral ligand loss step leaves the Au core incompletely protected (eq 3, $x = 8$, $y < 4$).

Minor product ions (not shown in Figure 4 to preserve clarity, see supplemental Figure 2), include $[Au_8L^5_3Ph_2P(CH_2)_5P]^{2+}$ (loss of two phenyl groups), $[Au_3L^5_2]^+$, $[Au_2L^5Ph]^+$, $[AuPh_2P$-

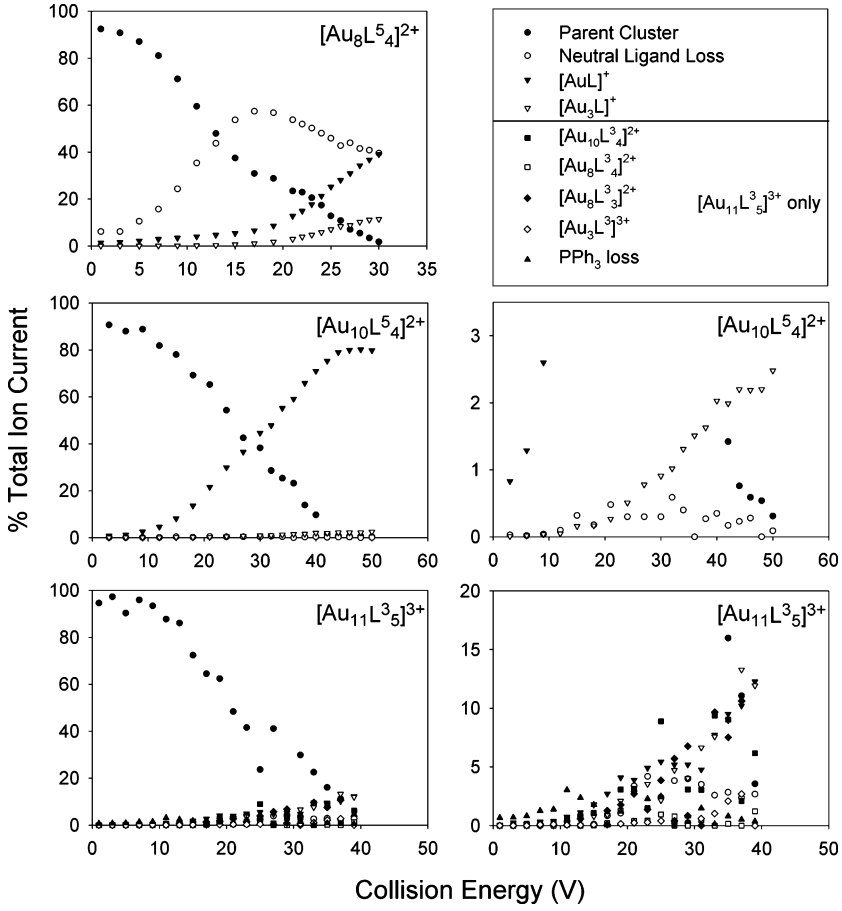

Figure 4. Branching ratios derived from CID of $[Au_8L^5_4]^{2+}$, $[Au_{10}L^5_4]^{2+}$, and $[Au_{11}L^3_5]^{3+}$, as labeled. The contribution of each ion to the total ion current is plotted against collision energy. For the deca- and undecagold clusters, magnified figures are shown on the right, so that trends in the minor channels are more visible. The legend gives the symbols for each loss channel. For undecagold, channels complementary to the prominent $[AuL]^+$ and $[Au_3L]^+$ channels are shown, as are an impartial ligand loss channel (PPh_3 loss) and the channel assigned as $[Au_3L^3]^{3+}$. The complexity of the undecagold portion of the figure illustrates that no dominant channel is present, and that multiple channels compete across the range of collision energies.

$(CH_2)_5]^+$, and $[AuPh_2P(CH_2)_5P]^{2+}$ (we do not suggest bonding in any of these formulas). The last two molecular product ions contribute less than 0.1% to the TIC, but merit mention due to their recurrence in the CID spectra of the other clusters. The Ph_2-loss channel is typical of a partial ligand loss (similar to eq 3), with a fairly high collision energy onset, and a steady rise to higher collision energies. The product ion with a gold dimer core ($[Au_2L^5Ph]^+$) is also fairly typical for the other clusters, again exhibiting a fairly high collision energy onset. The $[Au_3L^5_2]^+$ product ion is apparently unique to CID of the $[Au_8L^5_4]^{2+}$ cluster and is actually the most intense of the minor channels. It appears with a low collision energy onset and exhibits its maximum contribution to the TIC at about 25 V before tailing off at higher energies.

3.2.2. $[Au_{10}L^5_4]^{2+}$. The $[Au_{10}L^5_4]^{2+}$ cluster was found to be less susceptible to CID (both in-source and in the collision cell) than its octagold cousin. As Figure 4 shows, the most abundant product ion was $[AuL^5]^+$, which exhibits a low-energy onset and so can apparently arise as a primary fragment from the parent—that is, not necessarily the product of secondary fragmentation (eq 3, $x = 10$, $y = 4$). The inset of Figure 4 reveals the behavior of the product ions which were most prominent in the $[Au_8L^5_4]^{2+}$ case (eqs 1−3), of which $[Au_3L^5]^+$ is seen to be the most significant, displaying a steady rise across the collision energy range under scrutiny. The contribution from the neutral ligand loss channel (eq 1) is very weak (never exceeding 0.5% of the TIC), but a slight rise and fall is suggested. Many other minor contributions (see supplemental Figure 1) were observed, all of which correspond to partial ligand losses. In fact, it seems that neutral ligand loss, clearly an important first step in the fragmentation of $[Au_8L^5_4]^{2+}$, is often preempted by partial ligand loss from the parent $[Au_{10}L^5_4]^{2+}$ cluster (eq 5). Phenyl loss channels are particularly common in our data, and we conclude that the Au−P bonds of $[Au_{10}L^5_4]^{2+}$ are of comparable strength to the P−Ph bonds of the ligands. Interestingly, the product ion assigned as $[Au_2L^5Ph]^+$ shows a distinct rising and falling contribution to the TIC. It is difficult to refer to this species as an "important" product, given that its contribution to the TIC never exceeds 1%, but it may be that some of the smaller molecular product ions have passed through this intermediate.

3.2.3. $[Au_{11}L^3_5]^{3+}$. CID of the undecagold cluster proceeds in a manner somewhat similar to that of $[Au_{10}L^5_4]^{2+}$. $[AuL^3]^+$ is the most abundant product ion, and in this case the complementary $[Au_{10}L^3_4]^{2+}$ product ion can also be observed (eq 2). $[Au_3L^3]^+$ is observed (eq 3), with corresponding $[Au_8L^3_4]^{2+}$, as well as $[Au_8L^3_3]^{2+}$ (produced by a sequential reaction: eq 3, then eq 2). Neutral ligand loss (eq 1), leaving $[Au_{11}L^3_4]^{3+}$, appears, but at a collision energy threshold higher than for the $[AuL^3]^+$ channels. One non-negligible product ion (up to ~3% TIC) seems to be $[Au_3L^3]^{3+}$, which occurs at higher collision energies. No product ion ever exceeds a contribution of more than ~15% of the TIC, indicating that, as in the

decagold case, partial ligand losses lead to a spreading of the TIC over a wide sampling of the *m*/*z* range.

The product ion with the lowest energy onset corresponds to loss of PPh_3 (eq 4, although it is impossible to establish whether this is a bound triphenylphosphine neutral molecule, or multiple neutral fragments); the contribution from the $[Au_{11}L^3_4PPh(CH_2)_3]^{3+}$ product ion rises at low collision energies and then disappears at higher energies. The neutral ligand loss channel (eq 1) has a higher energy onset (~17 V), and its contribution to the TIC rises to about 4% at ~24 V before tailing off to higher energy. As the contribution from the neutral ligand loss channel begins to decline, a sharp rise in the $[AuL^3]^+$ channel (eq 2), which exhibits only a gradual increase before this energy threshold, is observed. We interpret this result as indicative that $[AuL^3]^+$ units are lost more easily from a cluster which has already lost one neutral ligand (eq 1, then eq 2); however, the low energy onset shows that the parent undecagold cluster (like the decagold cluster) can lose $[AuL^3]^+$ as a primary fragment (eq 2, $x = 11$, $y = 5$), leading here to production of the presumably stable $[Au_{10}L^3_4]^{2+}$ cluster. The channels involving loss of three Au atoms (eq 3) have a slightly higher energy onset than the $[AuL^3]^+$ channels, and show a gradual rise across the collision energy range. While loss of $[Au_3L^3]^+$ from the parent cluster leads directly to the stable $[Au_8L^3_4]^{2+}$ cluster, this appears to be a very weak channel (<1.5% TIC), and so it appears that $[Au_3L^3]^+$ (up to ≈ 14% TIC) arises mostly as a secondary fragment from clusters with incompletely protected cores (eq 3, $x \leq 11$, $y < 5$).

The appearance of the $[Au_{11}L^3_5]^{3+}$ branching ratio speaks to the stability of the cluster. It is difficult to follow any specific channel because so many channels compete at similar energies. The branching ratio for $[Au_8L^5_4]^{2+}$ shows very clear trends, easy to decipher. This is because specific bonds are particularly susceptible to cleavage, leading to an energetic preference for certain fragmentation pathways. When no specific pathway is favored over another, trends in the branching ratio are more difficult to identify; in the case of $[Au_{11}L^3_5]^{3+}$, competition between channels indicates a particularly stable core configuration in that cleavage of ligand−core bonds competes energetically with cleavage of intraligand bonds. Similarly, in figure S1, the branching ratio for $[Au_{10}L^5_4]^{2+}$ is more difficult to follow than that for $[Au_8L^5_4]^{2+}$.

4. Discussion

4.1. Solvent Mediation of Cluster Formation. The greater solubility in polar solvents of Au MPCs with smaller cores is, by now, a well-known empirical property,[4,22−24] forming the basis for the fractional crystallization techniques that enable quantitative separations of alkanethiol protected clusters. For MPCs with alkanethiol protecting layers, variations in both core size and ligand properties lead to drastic differences in particle solubility. Donkers et al. have noted that the solvation characteristics of thiolate ligands are important in the search for new MPC core sizes.[22] Solubility trends have been attributed to polar Au−ligand interactions, as well as to solvent penetration effects, but to our knowledge, no detailed understanding of the empirical observations has yet been synthesized.

The clusters under scrutiny in the present work have several unique properties that might complicate particle−solvent interactions. First, while alkanethiol protected clusters are thought to have an essentially neutral Au(0) core, and most small phosphine protected clusters feature pseudohalide ligands to balance the gold core's intrinsic charge, the diphosphine protected clusters are putatively charged in solution. Ion solvation typically involves much stronger intermolecular interactions than neutral solvation, and so our situation might not be very analogous to the alkanethiol one. It is possible that contact ion ensembles exist within the solution (a cationic cluster surrounded by anionic counterions), in which case the entire unit might be treated as a polar salt molecule, but we have no evidence to support this hypothesis. Recently, Yanagimoto et al.[15] reported that while $[Au_{11}(PPh_3)_8Cl_2]^+$ clusters actually undergo chemical degradation in MeOH, $[Au_{11}(BINAP)_4Br_2]^+$ (BINAP = 2,2′-bis(diphenylphosphino)-1,1′-binaphthyl) clusters do not. While the exact reaction mechanisms for degradation of the Au:PPh_3 clusters was uncertain, ESI-MS indicated that $Au_{10}(PPh_3)_8$-based ions represented major degradation products. They suggested that the bidentate nature of the ligand offers improved resistance to degradation in MeOH. While the mechanisms remain uncertain, our observations on the synthesis and ESI-MS of small diphosphine protected gold clusters indicate that improved solubility in a polar medium can play an important role in the formation of MPCs.

Improved solubility of the clusters in MeOH has two major effects on our synthetic endeavors: (1) the reaction proceeds more rapidly as a result of the lower energy state of the products; (2) the increased solvation energy of the clusters will necessarily be a general property of many protected clusters with charged cores, and thus synthetic monodispersity will be affected. The first point explains that our reaction generates products within ~10 min in mixed solvent environments as opposed to several hours in pure chloroform. This is simply a matter of stabilizing the products. In the popular model of MPC formation, the reduction of the gold precursors is performed in the presence of labile ligands; at certain kinetically or thermodynamically favored points in the reaction, the ligands effectively cease to be labile, and thus inhibit further core growth. Essentially, the presence of MeOH in the solution serves to deepen the potential energy well of the products (through increased solvation energy), thus driving the reaction downhill and trapping it at the stable sizes. At the same time, the polar solvent environment makes it energetically unfavorable for the ligands to be in solution, so that their association to clusters is preferred. Similarly, point two is related to the deepening of potential energy wells. The monodispersity of the synthesis is adversely affected by the presence of MeOH in the reaction solution, as is evidenced in Figure 2, where small amounts of $[Au_6L^3_3]^{2+}$ (apparently completely coordinated, but interestingly having one bidentate ligand less than a known stable $[Au_6L^3_4]^{2+}$ hexagold cluster[17]) and $[Au_8L^3_4]^{2+}$ appear in addition to the desired $[Au_{11}L^3_5]^{3+}$. In this case, it can be seen that the formation of the undecagold cluster relies on the thermodynamic instability (meaning the ligands are still labile) of the hexa- and octanuclear gold cluster intermediates. Because the ligands are less labile in a more polar solvent environment, and because of the deepening the potential energy wells of the clusters, quantities of these intermediates are preserved in the final product sample. It is possible that with a dedicated effort, a more ideal solvent could be identified in order to strike a perfect balance between cluster stability, formation rate, and synthetic specificity.

To briefly address the emergence of the octa- and decanuclear clusters as predominant over the enneanuclear species, we note that because the undecagold cluster is found to be readily synthesized with L^3, a mechanistic argument involving cluster formation from dimer units seems unreasonable. Instead, it seems likely that energetic factors arising from the strain imparted on the D_{4d} Au_9 core[17] by the bidentate ligands, leads to the observed disproportionation. The only small cluster that

might be a building block for nanoparticle formation is the trinuclear gold cluster, but we have no strong evidence to suggest that cluster coalescence plays a major role in nanoparticle formation. We find it perfectly plausible that the main growth mechanism involves solely mononuclear units.

Finally, cluster stabilization via solvation is evidenced by the improved shelf life of MeOH-dissolved samples. Despite the diphosphine protecting layer, clusters stored in $CHCl_3$ are susceptible to oxidation. However, when stored in MeOH, no sample degradation is observed. This is a result of the improved protection offered by a stronger cluster-solvent interaction, combined with the diminished ligand-solvent interaction which makes the ligands far less labile.

4.2. CID of MPCs. For each cluster considered, only one neutral ligand loss is observed, after which core fission is the preferred fragmentation pathway.[25] This is in contrast to the observations of Zhang et al.,[2] where up to four neutral ligand losses were observed from $[Au_{20}(PPh_3)_8]^{2+}$.[26] For our small clusters, then, core stabilization requires an exact stoichiometric balance between Au atoms and ligand molecules; in other words, while the results of Zhang et al. establish that preservation of a Au_{20}^{2+} core is possible with labile ligands,[2] our results show that the smaller clusters are only stable with their complete complement of ligands. Until a thermodynamically preferred stoichiometry is achieved, the gold atoms are not strongly bound to the cluster, and are likely as labile as the ligands.

Of course, neutral ligand loss is not equally efficient for each of the clusters described herein. While facile for $[Au_8L^5_4]^{2+}$, neutral ligand loss from $[Au_{10}L^5_4]^{2+}$ and $[Au_{11}L^3_5]^{3+}$ is less pronounced and partial ligand losses are common instead. Several factors differentiate the two types of cluster. First, while the decagold cluster has two Au atoms that are not bound to P and the undecagold cluster has one, every Au atom is bound to P in the octagold cluster. That is, the surface:volume ratio varies from 10:1 to 8:2 to 8:0 for $[Au_{11}L^3_5]^{3+}$, $[Au_{10}L^5_4]^{2+}$, and $[Au_8L^5_4]^{2+}$, respectively; this undoubtedly has an effect on the observed chemistry. In addition, it has been suggested that the stability of the deca- and undecagold clusters arises from the preference for an eight electron gold cluster core. The octagold cluster, which does not have an eight electron core, might therefore be predicted to be more weakly bound. We are unaware of any theoretical or experimental investigations which might establish why an electronically stable gold core would lead to stronger Au−P interactions, but it is possible that this phenomenon is related to the polarity (or charge transfer) of the chemical bonds. Ligand interactions certainly have a strong effect on the geometric and electronic properties of the gold core, making comparisons to bare clusters—which have received extensive theoretical and experimental attention—invalid.

Several other features of the CID data allow us to glean structural information on the clusters. First, we consider the initial loss channels. The lowest energy fragmentation events involve complete or partial neutral ligand losses. No charged ligand or ligand fragments appear, confirming that the charge is centralized on the gold core in all of the clusters we have considered. Second, we consider that the absence of any Au^+ is evidence for well protected cluster cores. Finally, and more subtly, the absence of an Au_2L loss channel provides evidence for a gross structural deformation upon cleavage of an Au−L bond. Because each ligand is thought to be bound to two Au atoms on a cluster surface, one would expect that if the cluster structure were preserved in the fragmentation process, then Au_2L loss would be an important fragmentation channel. Instead, it is clear that the initial cleavage of one Au−P bond leads to a deformation of sufficient magnitude as to promote (mostly) either $[AuL]^+$ or $[Au_3L]^+$ loss. We are currently undertaking a series of theoretical investigations designed to offer a detailed description of the mechanisms involved in this process. These investigations also seek to explain the prevalence of the unexpectedly prominent $[Au_3L]^+$ fission product. As this product ion appears in the CID of every cluster we studied, we can safely conclude that the intrinsic stability of $[Au_3L]^+$, and not of a remaining ion, leads to its ubiquity. It is possible that such a thermodynamically stable species would serve as a major building block for the formation of larger MPCs.

5. Conclusions

We have presented a modified synthesis of diphosphine-protected gold nanoparticles, which adds MeOH to the reaction solution to stabilize the MPC products. Compared to the procedure reported by Bertino et al.,[13] our simple method enables a much more rapid synthesis, prolongs shelf life, and facilitates more stable ion current from ESI. The improved ion currents enable CID studies, which give more detail on the properties of the specific clusters of interest. Neutral ligand loss constitutes an important first step for the dissociation of $[Au_8L^5_4]^{2+}$, while for the more strongly bound $[Au_{10}L^5_4]^{2+}$ and $[Au_{11}L^3_5]^{3+}$ clusters, partial ligand loss is prevalent. The decagold cluster is much more resistant to CID than the octagold cluster, which appears in the same mass spectrum. Thus, partial ligand losses from the more stable decagold and undecagold clusters indicate stronger Au−P interactions in the more stable clusters. For all of the clusters, $[AuL]^+$ and $[Au_3L]^+$ are important product ions; the removal of just one protecting ligand leaves the gold cores of these small MPCs susceptible to fission, although fission as a primary fragmentation event is possible from $[Au_{10}L^5_4]^{2+}$ and $[Au_{11}L^3_5]^{3+}$. Future studies will seek to provide a more comprehensive picture of core-ligand interactions with varying core size and ligand functionality.

Acknowledgment. We acknowledge invaluable experimental assistance from Pedatsur Neta. We thank Vladimir Orkin for providing access to the UV−vis spectrophotometer, Xiaoyu (Sara) Yang for providing software assistance for data analysis, and Bianca Hydutsky for useful discussions.

Supporting Information Available: Figure S1 shows the low % TIC portion of the branching ratios derived from CID of $[Au_8L^5_4]^{2+}$ and $[Au_{10}L^5_4]^{2+}$. Tables S1, S2, and S3 show typical raw data for the CID of $[Au_8L^5_4]^{2+}$, $[Au_{10}L^5_4]^{2+}$, and $[Au_{11}L^3_5]^{3+}$, respectively. This material is available free of charge via the Internet at http://pubs.acs.org.

References and Notes

(1) Daniel, M. C.; Astruc, D. *Chem. Rev.* **2004**, *104*, 293.
(2) Zhang, H. F.; Stender, M.; Zhang, R.; Wang, C. M.; Li, J.; Wang, L. S. *J. Phys. Chem. B* **2004**, *108*, 12259.
(3) Fackler, J. P.; McNeal, C. J.; Winpenny, R. E. P.; Pignolet, L. H. *J. Am. Chem. Soc.* **1989**, *111*, 6434.
(4) Whetten, R. L.; Khoury, J. T.; Alvarez, M. M.; Murthy, S.; Vezmar, I.; Wang, Z. L.; Stephens, P. W.; Cleveland, C. L.; Luedtke, W. D.; Landman, U. *Adv. Mater.* **1996**, *8*, 428.
(5) Alvarez, M. M.; Khoury, J. T.; Schaaff, T. G.; Shafigullin, M. N.; Vezmar, I.; Whetten, R. L. *J. Phys. Chem. B* **1997**, *101*, 3706.
(6) Schaaff, T. G.; Knight, G.; Shafigullin, M. N.; Borkman, R. F.; Whetten, R. L. *J. Phys. Chem. B* **1998**, *102*, 10643.
(7) Schaaff, T. G.; Whetten, R. L. *J. Phys. Chem. B* **2000**, *104*, 2630.
(8) Negishi, Y.; Takasugi, Y.; Sato, S.; Yao, H.; Kimura, K.; Tsukuda, T. *J. Am. Chem. Soc.* **2004**, *126*, 6518.
(9) Negishi, Y.; Tsukuda, T. *Chem. Phys. Letters* **2004**, *383*, 161.
(10) Negishi, Y.; Nobusada, K.; Tsukuda, T. *J. Am. Chem. Soc.* **2005**, *127*, 5261.

(11) Shichibu, Y.; Negishi, Y.; Tsukuda, T.; Teranishi, T. *J. Am. Chem. Soc.* **2005**, *127*, 13464.
(12) Negishi, Y.; Takasugi, Y.; Sato, S.; Yao, H.; Kimura, K.; Tsukuda, T. *J. Phys. Chem. B* **2006**, *110*, 12218.
(13) Bertino, M. F.; Sun, Z. M.; Zhang, R.; Wang, L. S. *J. Phys. Chem. B* **2006**, *110*, 21416.
(14) Schaaff, T. G.; Whetten, R. L. *J. Phys. Chem.* B **1999**, *103*, 9394.
(15) Yanagimoto, Y.; Negishi, Y.; Fujihara, H.; Tsukuda, T. *J. Phys. Chem. B* **2006**, *110*, 11611.
(16) Smits, J. M. M.; Bour, J. J.; Vollenbroek, F. A.; Beurskens, P. T. *J. Crystallogr. Spectrosc. Res.* **1983**, *13*, 355.
(17) Hall, K. P.; Mingos, D. M. P. *Prog. Inorg. Chem.* **1984**, *32*, 237.
(18) Certain commercial equipment, instruments, or materials are identified in this paper to foster understanding. Such identification does not imply recommendation or endorsement by the National Institute of Standards and Technology, nor does it imply that the materials or equipment identified are necessarily the best available for the purpose.
(19) Nanfeng, Zheng, J. F.; Stucky, G. D. *J. Am. Chem. Soc.* **2006**, *128*, 6550.
(20) Of course, lab-to-lab comparisons of mass spectral data are difficult, and the triple quadrupole instrument that we used in the current studies will differ dramatically, particularly with respect to collision conditions, from the ion cyclotron resonance mass spectrometer employed by Bertino et al.
(21) Colton, R.; Harrison, K. L.; Mah, Y. A.; Traeger, J. C. *Inorg. Chim. Acta* **1995**, *231*, 65.
(22) Donkers, R. L.; Lee, D.; Murray, R. W. *Langmuir* **2004**, *20*, 1945.
(23) Hicks, J. F.; Templeton, A. C.; Chen, S. W.; Sheran, K. M.; Jasti, R.; Murray, R. W.; Debord, J.; Schaaf, T. G.; Whetten, R. L. *Anal. Chem.* **1999**, *71*, 3703.
(24) Schaaff, T. G.; Shafigullin, M. N.; Khoury, J. T.; Vezmar, I.; Whetten, R. L. *J. Phys. Chem. B* **2001**, *105*, 8785.
(25) For bare metal clusters, the loss of one metal atom is typically referred to as "evaporation", and the word "fission" is reserved for events in which multiple metal atoms are lost. For MPCs, "evaporation" would seem to imply ligand dissociation, and so we use "fission" to refer to any loss of core metal atoms.
(26) Given that the ligands considered in the present work are bidentate, the four neutral ligand losses observed by Zhang et al. [ref 2] would correspond to only two ligand losses from our clusters. Still, this was not observed. Possibly, this is related to the binding of phosphines to face sites of Au_{20}. Such face sites are not present on the small clusters treated herein.